Supporting Information

Recognizing the important role of surface barriers in MOR zeolite catalyzed DME carbonylation reaction

Kaipeng Cao[a, b], *Dong Fan*[a], *Mingbin Gao*[a], *Benhan Fan*[a, b], *Nan Chen*[a, b], *Linying Wang*[a], *Peng Tian*[*, a] *and Zhongmin Liu*[*, a]

[a] National Engineering Laboratory for Methanol to Olefins, Dalian National Laboratory for Clean Energy, Dalian Institute of Chemical Physics, Chinese Academy of Sciences, Dalian 116023, China.

[b] University of Chinese Academy of Sciences, Chinese Academy of Sciences, Beijing 100049, China.

*Corresponding authors: tianpeng@dicp.ac.cn; liuzm@dicp.ac.cn

EXPERIMENTAL SECTION

Materials and reagents

Sodium hydroxide (NaOH, 99.9 wt%, Shanghai Aladdin Industrial Co.); sodium aluminate ($NaAlO_2$, 36.6 wt% Na_2O, 47.6 wt% Al_2O_3, Tianjin Guangfu Chemical Co.); silica sol (27.5 wt% SiO_2, Qingdao Chengyu Chemical Co.); tetraethylammonium hydroxide (TEAOH, 35 wt% in H_2O, Shanghai Annaiji Chemical Reagent Co.); cyclohexylamine (CHA, 99 wt%, Shanghai Annaiji Chemical Reagent Co.); trimethylamine (TMA, 40 wt% in H_2O, Shanghai Annaiji Chemical Reagent Co.); hydrofluoric acid solution (40 wt%, Sigma-Aldrich (Shanghai) Trading Co.Ltd); acetone (99.9 wt%, Sigma-Aldrich (Shanghai) Trading Co.Ltd).

Zeolites synthesis and catalyst preparation

A hydrothermal synthesis method was carried out for the preparation of MOR zeolites. NaOH, $NaAlO_2$, OSDAs, and H_2O were first introduced into a beaker at room temperature and stirred until dissolved completely. Silica sol was then introduced in drops under intense agitation. Subsequently, commercial MOR zeolite used as a seed (4 wt% relative to SiO_2) was added into the above mixture. The specific compositions of the synthetic gel have been shown in Table S1 After aging for 1 h under stirring, the final gel was transferred into an autoclave (100 mL) and heated under static conditions at 170 ^oC for 20 hours. Afterward, the crystallized product was washed with distilled water and centrifuged for recovery, then dried at 120 ^oC.

In order to obtain H-type MOR, the as-made samples were first calcined at 550 °C. Subsequently, the calcined samples were ion-exchanged with NH_4NO_3 solution (1 mol/L, 80 ^oC for 1h). The ion-exchange procedure was repeated three times and dried at 120 ^oC. Finally, the exchanged sample was calcined at 550 °C for 4 h under dry air.

Surface etching in acetone-HF solution

The surface etching treatment of the as-made MOR zeolite was carried out following the strategy reported previously[1-2]. 3 g of as-made sample and 9.6 g of acetone were first introduced into a Teflon container, and stirred for 10 min. Then, 2.5 g of HF solution (10 wt%, obtained by mixing 40 wt% HF

aqueous solution with acetone) was added to the suspension. The suspension underwent further agitation for 5 min. Finally, the sample was thoroughly washed and dried at 120 ^{o}C. The etched two samples were denoted as MOR-C-F and MOR-T-F.

Acid etching

MOR-C1-a1: MOR-C1 (sample 14 in Table S6) was treated by citric acid solution (0.5 mol/L) at 50 ^{o}C for 12 h under stirring (solid/liquid = 1 g/10 g); MOR-C1-a2: MOR-C1 was treated by citric acid solution (0.5 mol/L) at 80 ^{o}C for 6 h under stirring (solid/liquid = 1 g/10 g); MOR-C1-a3: MOR-C1 was treated by citric acid solution (1 mol/L) at 80 ^{o}C for 12 h under stirring (solid/liquid = 1 g/10 g); After the treatment, the sample was thoroughly washed and dried at 120 ^{o}C.

Alkali etching

MOR-C1-b1: MOR-C1 was treated with TEAOH solution (0.5 mol/L) at 50 ^{o}C for 12 h under stirring (solid/liquid = 1 g/10 g); MOR-C1-b2: aMOR-C1 was treated with TEAOH solution (0.5 mol/L) at 80 ^{o}C for 6 h under stirring (solid/liquid = 1 g/10 g); MOR-C1-b3: MOR-C1 was treated with TEAOH solution (1 mol/L) at 80 ^{o}C for 12 h under stirring (solid/liquid = 1 g/10 g). After the treatment, the sample was thoroughly washed and dried at 120 ^{o}C.

(Co, Na)-MOR samples preparation

(Co, Na)-MOR samples were prepared by following the procedures reported[3-5], which could avoid the formantion of bridging and isolated cobalt oxides. The calcined sample was first ion-exchanged to Na-MOR with a $NaNO_3$ aqueous solution (1 mol/L, 80 °C for 12 h). Subsequently, the obtained Na-MOR was ion exchanged with a $Co(NO_3)_2$ aqueous solution (0.05 mol/L) at room temperature for 24 h. This Co^{2+}-exchange procedure was repeated three times. After ion-exchange, the samples were washed with deionized water and recovered by centrifugation.

Catalyst characterization

X-ray diffraction (XRD) patterns were obtained on an X-ray diffractometer of PANalytical X'Pert PRO with Cu Kα radiation (scanning region: 5~50^{o}). The morphologies of zeolites were acquired using JEOL JEM-2100 transmission electron microscopy (TEM) and Hitachi SU8020 scanning electron microscope (SEM). Textural properties of the samples were obtained on a Micromeritics ASAP 2020 analyzer through N_2 adsorption and desorption measurements. The OSDAs content of as-made MOR zeolites and pyridine content in pyridine-modified catalysts were determined on a TA Q-600 thermogravimetric analyzer (TG). The bulk Si/Al ratios were measured on an X-ray fluorescence (XRF)

spectrometer of Philips Magix-601. The surface Si/Al ratios were determined using an EscaLab 250Xi X-ray photoelectron spectroscopy (XPS). Temperature programmed desorption of NH_3 (NH_3-TPD) was performed on a Micromeritics Autochem II 2920. A Bruker Tensor 27 spectrometer (MCT detector) was adopted for the measurement of fourier transform infrared spectra (FTIR). The MOR samples were pressed self-supported wafers and placed into the in situ quartz cell. Subsequently, the wafers were dehydrated at 400 °C in a vacuum for 30 min to remove the water physisobed. After cooling to room temperature, the spectra were collected by a MCT detector in the range of 400–4000 cm^{-1} with a resolution of 4 cm^{-1}. ^{27}Al, ^{29}Si and ^{1}H MAS NMR spectra were recorded on a Bruker Avance III 600 MHz spectrometer. ^{27}Al spectra were collected at 156.4 MHz with a spinning rate of 12 kHz, a recycle delay of 2 s and π/8 pulse width of 0.75 μs. ^{29}Si spectra were recorded at 119.2 MHz with a π/4 pulse width of 2.5 μs, a 10 s recycle delay and an 8 kHz spinning rate. Prior to ^{1}H MAS NMR investigation, H-MOR samples were dehydrated at 420 °C under vacuum for 20 h to remove the water physisobed. The spectra were then recorded at 600.13 MHz with a π/2 pulse of 3.2 μs, a recycle delay of 10 s and a 20 kHz spinning speed using a Hahn-Echo pulse sequence. The chemical shifts were referenced to adamantane at 1.74 ppm.

Uptake of n-butane

The uptake rates of butane in H-MOR samples were measured on an intelligent gravimetric analyzer (IGA). Samples (appr. 25 mg, 40-60 mesh) were first outgassed at 300 °C until a constant weight reached. The butane vapor was then introduced to the chamber and the adsorption kinetics curves were recorded at 30 °C and 5 mbar. The surface barriers and intracrystalline diffusion of guest molecules were quantified through the dual resistance model (DRM) [6].

$$\frac{m_t}{m_\infty} = 1 - \sum_{n=1}^{\infty} \frac{2L^2 \exp\left(-\frac{\beta_n^2 D t}{l^2}\right)}{(\beta_n^2 + L^2 + L)\beta_n^2}; \qquad \beta_n \tan \beta_n = L = \frac{\alpha l}{D} \tag{1}$$

where m_t/m_∞ is the normalized loading, t the uptake time, D the intracrystalline diffusivity, α the surface permeability, and l the equivalent radius. α is estimate from the initial uptake rate following Gao et al [7-8].

$$\frac{m_t}{m_\infty} \Big|^{\sqrt{t}\to 0} = \frac{\alpha}{l}(\sqrt{t})^2 \tag{2}$$

Uptake of methyl acetate (MAc)

The uptake rates of MAc on pyridine-modified H-MOR catalysts were measured on an Intelligent

Gravimetric Analyzer (IGA). Samples (appr. 25 mg, 40-60 mesh) were first outgassed at 300 °C until a constant weight reached. The MAc vapor was then introduced to the chamber and the adsorption kinetics curves were recorded at 50 °C and 1 mbar.

Fick's second law was used to quantify the effective diffusivity, and the variation of the MAc concentration with time inside the pyridine-modified catalysts can be described as follows[9-11].

$$\frac{\partial C}{\partial t} = D_{eff}\left(\frac{\partial^2 C}{\partial x^2}\right) \qquad (3)$$

Where x, t, C and D_{eff} represent the diffusion distance, diffusion time, MAc concentration inside the particle, and the diffusivity, respectively. In the initial stage of uptake, the solution of this equation can be approximated as follows:

$$\frac{m_t}{m_\infty} = \frac{2}{\sqrt{\pi}}\sqrt{\frac{D_{eff}}{L^2}}\sqrt{t} \qquad (4)$$

Where L, t and m_t/m_∞ are the characteristic diffusion length, diffusion time and the normalized MAc uptake, respectively.

Toluene adsorption

The toluene adsorption isotherms were measured by IGA. The H-MOR sample was loaded in the chamber and evacuated at 400 °C for 1 h. The mass variation following the adsorption of toluene over H-MOR was measured at 31.7 °C with increasing pressures (0→50 mbar).

Catalytic testing

DME carbonylation

The DME carbonylation activity and stability of catalysts were evaluated in a fixed bed reactor. The H-MOR samples (0.25 g, 40-60 mesh) were pretreated with N_2 in the reactor at 400 °C for 2 h. Afterwards, the temperature was reduced to 300 °C, the sample was purged with a pyridine-N_2 mixture (30 mL/min) for 20 min and then flushed with N_2 for 1 h. When the temperature was cooled to reaction temperature (200 or 220 °C), a mixture of reactant gas (DME: CO: N_2 = 5: 35: 60) was introduced. The reaction was carried out at 2.0 MPa with a GHSV of 3600 or 12000 mL/g/h. The products analysis was carried out using an Agilent 7890B gas chromatograph equipped with Pora PLOT Q capillary column and FID detector.

Isopropyl benzene (IPB) cracking

IPB cracking was performed in a fixed-bed quartz tubular reactor at atmospheric pressure. 50 mg of

the catalyst (40-60 mesh) diluted by 0.50 g quartz was loaded into the reactor and activated in N_2 (40 Ml/min) at 300 ^oC for 1 h prior to the reaction. N_2 (40 mL/min) saturated with vaporized IPB at 40 ^oC was passed through the reactor, which gave an IPB WHSV of 3.4 h^{-1} and the reaction temperature was 210 ^oC. The effluents from the reactor were kept at 200 °C and analyzed using an online Agilent 7890A GC equipped with a PONA capillary column (100 m × 0.25 mm × 0.5μm) and a FID detector.

1,3,5-triisopropylbenzene (TIPB) cracking

TIPB cracking was performed in a fixed-bed quartz tubular reactor at atmospheric pressure. For each experiment, 30 mg of the catalyst (40-60 mesh) diluted by 0.50 g quartz was loaded into the reactor, and dehydrated in N_2 (40 mL/min) at 300 ^oC for 1 h prior to the reaction. The temperature of the catalyst bed was then maintained at 300 ^oC. TIPB was fed by passing the carrier gas (N_2, 100 mL/min) through a saturator containing TIPB at 70 ^oC, which gave a TIPB WHSV of 4.1 h^{-1}. The effluents from the reactor were kept at 200 °C and analyzed using an online Agilent 7890A GC equipped with a PONA capillary column (100 m × 0.25 mm × 0.5μm) and a FID detector.

N-octane cracking

0.10 g of catalyst (40-60 mesh) was placed in a fixed bed quartz tubular reactor and activated under N_2 (40 mL/min) at 500 °C for 30 min, and then the temperature was maintained at 500 ^oC. The reaction was conducted under atmospheric pressure. N-octane was fed by passing the N_2 (40 mL/min) through a saturator containing n-octane at 60 ^oC, which gave a n-ocane WHSV of 11.6 h^{-1}. The effluents from the reactor were kept at 200 °C and analyzed by an online Agilent 7890A GC equipped with a HP-1 capillary column (100m×0.25mm×0.5μm) and a FID detector.

Table S1 Molar compositions of the initial gels for the synthesis of MOR zeolites

Sample	SiO_2	Al_2O_3	Na_2O	Trimethylamine	TEAOH	CHA	H_2O
MOR-T	30	1.0	3.0	3	3.0	0	480
MOR-C	30	1.0	3.0	0	0	6	480

Table S2 Textural properties and chemical compositions of the samples

Sample	Si/Al ratio		Surface area (m^2 g^{-1})			Pore volume (cm^3 g^{-1})		
	XRF[a]	XPS[b]	S_{ext}[c]	S_{micro}[d]	S_{BET}[e]	V_{meso}[f]	V_{micro}[g]	V_{total}[h]
MOR-T	13.4	14.5	48	366	414	0.04	0.18	0.22
MOR-C	13.6	15.3	42	314	356	0.05	0.15	0.20
MOR-C-F	13.5	15.6	45	315	360	0.06	0.15	0.21

[a]Derived from XRF analysis of as-made samples. [b]Derived from XPS analysis of as-made samples. [c]S_{ext}: external surface area. [d]S_{micro}: t-plot micropore surface area. [e]S_{BET}: BET surface area. V_{meso}: mesoporous volume. V_{micro}: t-plot micropore volume. V_{total}: total volume absorbed at P/P_0=0.99. $S_{ext} = S_{BET} - S_{micro}$. [d]$V_{total}$, $V_{meso} = V_{total} - V_{micro}$.

Table S3 Acid quantity and distribution derived from NH_3-TPD, ^{1}H MAS NMR and FTIR.

Sample	NH_3-TPD (mmol/g)				^{1}H NMR (mmol/g)	FTIR (%)
	Weak	Moderate	Strong	M+S[a]	Total BAS[b]	BAS of 8-MR[c]
MOR-T	0.51	0.18	0.68	0.86	0.64	45
MOR-C	0.51	0.22	0.63	0.85	0.57	46

MOR-C-F	0.52	0.17	0.65	0.82	-	45

[a]M+S = Moderate+Strong. [b]Total BAS: the total Brønsted acid sites density, calculated based on ^{1}H NMR results. [c]BAS of 8-MR: the ratio of Brønsted acid sites in 8-MR channel, derived from FTIR.

Table S4 Relative percentage of Si-(OH)-Al, Al-OH and Si-OH calculated based on the deconvoluted ^{1}H MAS NMR spectra

Sample	Relative percentage (%)		
	Si-(OH)-Al	Al-OH	Si-OH
MOR-T	64.2	19.8	16.0
MOR-C	77.2	16.3	6.5

Table S5 Effect of gel Na_2O amount on the synthesis

Sample	Starting gel (in mole)					Crystallization time/h	Product	
	SiO_2	Al_2O_3	Na_2O	OSDA	H_2O		Phase	Si/Al ratio
1	30	1	2.1	C[a]	480	48	Amorphous+MOR	-
2	30	1	2.4	C	480	36	MOR+MFI	-
3	30	1	2.7	C	480	24	MOR+MFI	-
4 (MOR-C)	30	1	3.0	C	480	20	MOR	13.6
5	30	1	3.6	C	480	16	MOR	12.7
6	30	1	4.2	C	480	12	MOR	11.2
7	30	1	2.1	T[b]	480	48	MOR	-
8	30	1	2.4	T	480	24	MOR	14.5
9 (MOR-T)	30	1	3.0	T	480	20	MOR	13.4
10	30	1	3.6	T	480	16	MOR	-
11	30	1	4.2	T	480	12	MOR	-

[a] 6 cyclohexylamine (CHA); [b] 3 tetraethylammonium hydroxide (TEAOH) + 3 trimethylamine (TMA); Synthesis conditions: crystallization at 170 ^{o}C under static condition.

Table S6 Effect of gel Si/Al ratio on the synthesis

Sample	Starting gel (in mole)					Crystallization time/h	Product	
	SiO_2	Al_2O_3	Na_2O	OSDA	H_2O		Phase	Si/Al ratio
12	30	1.5	3.0	C[a]	480	36	MOR	10.1
13	30	1.25	3.0	C	480	24	MOR	11.4
14 (MOR-C1)	30	1.0	3.0	C	480	24	MOR	13.7
15	30	0.9	3.0	C	480	20	MOR+MFI	-
16	30	0.8	3.0	C	480	20	MOR+MFI	-
17	30	1.5	2.4	T[b]	480	36	MOR	9.9
8	30	1.0	2.4	T	480	24	MOR	14.5
18	30	0.8	2.4	T	480	20	MOR	16.4
19	30	0.7	2.4	T	480	20	MOR	17.8
20	30	0.5	2.4	T	480	20	MOR	21.9

[a] 6 cyclohexylamine (CHA); [b] 3 tetraethylammonium hydroxide (TEAOH) + 3 trimethylamine (TMA); Synthesis conditions: crystallization at 170 °C under static condition.

Table S7 Effect of OSDA amount on the synthesis

Sample	Chemical composition of starting gel					Crystallization time/h	Product Phase
	SiO_2	Al_2O_3	Na_2O	OSDA	H_2O		
21	30	1	3.0	5CHA	480	36	MOR+MFI
14 (MOR-C1)	30	1	3.0	6CHA	480	24	MOR
22	30	1	3.0	9CHA	480	24	MOR
23	30	1	2.4	2TEAOH+0TMA	480	36	MOR
24	30	1	2.4	2TEAOH+2TMA	480	36	MOR
8	30	1	2.4	3TEAOH+3TMA	480	24	MOR

Synthesis conditions: crystallization at 170 °C under static condition.

Table S8 Effect of gel H_2O amount on the synthesis

Sample	Starting gel (in mole)					Crystallization time/h	Product	
	SiO_2	Al_2O_3	Na_2O	OSDA	H_2O		Phase	Si/Al ratio
25	30	1	3.0	C[a]	390	24	MOR+MFI	-
14 (MOR-C1)	30	1	3.0	C[a]	480	24	MOR	13.7
26	30	1	3.0	C	600	32	MOR	13.3
27	30	1	3.0	C	900	48	Amorphous+MOR	-
28	30	1	2.4	T	390	24	MOR	-
8	30	1	2.4	T	480	24	MOR	14.5
29	30	1	2.4	T	600	32	MOR	14.1
30	30	1	2.4	T	900	48	Amorphous+MOR	-

[a] 6 cyclohexylamine (CHA); [b] 3 tetraethylammonium hydroxide (TEAOH) + 3 trimethylamine (TMA); Synthesis conditions: crystallization at 170 °C under static condition.

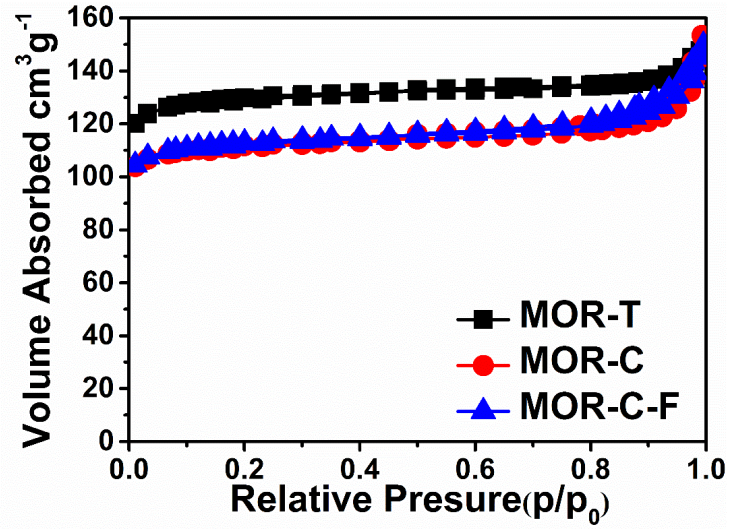

Figure S1 N_2 adsorption-desorption isotherms of the H-MOR samples.

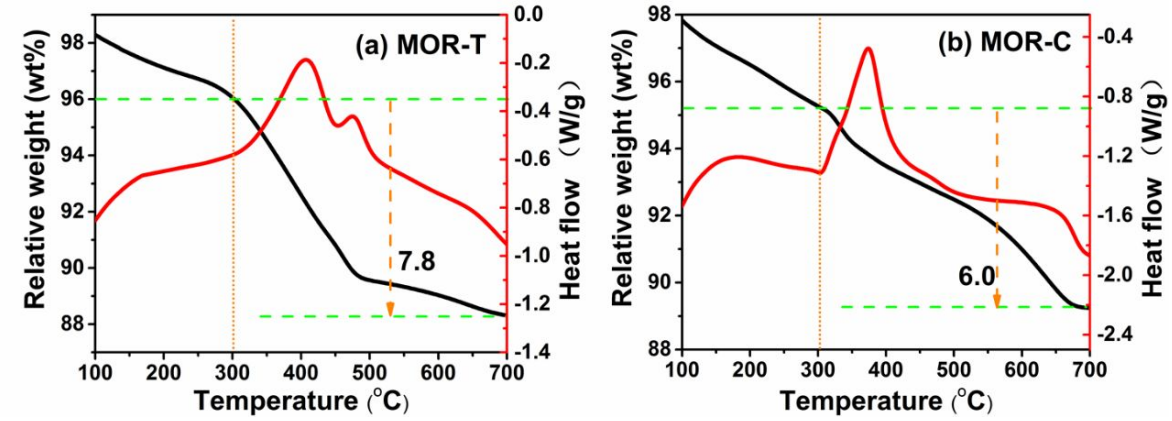

Figure S2 Thermal analysis profiles of the as-made MOR samples.

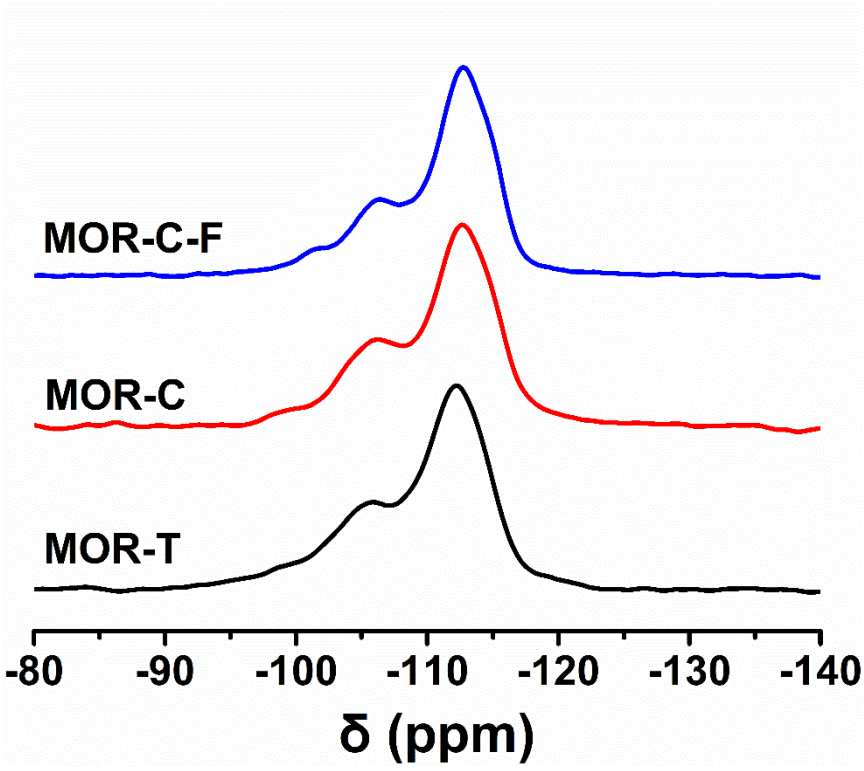

Figure S3 ^{29}Si MAS NMR spectra of the as-made samples.

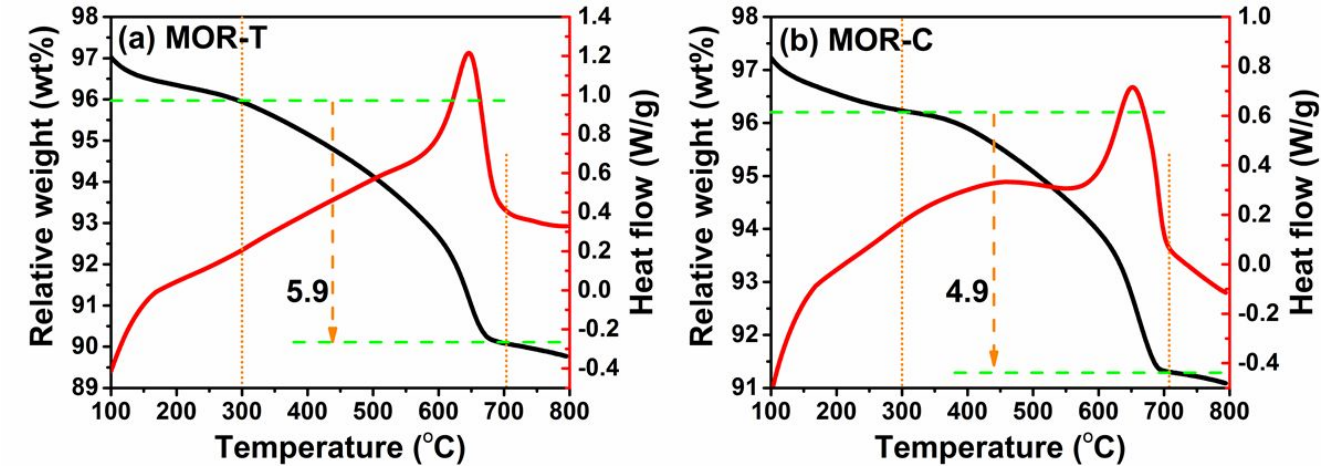

Figure S4 Thermal analysis profiles of pyridine modified H-MOR samples.

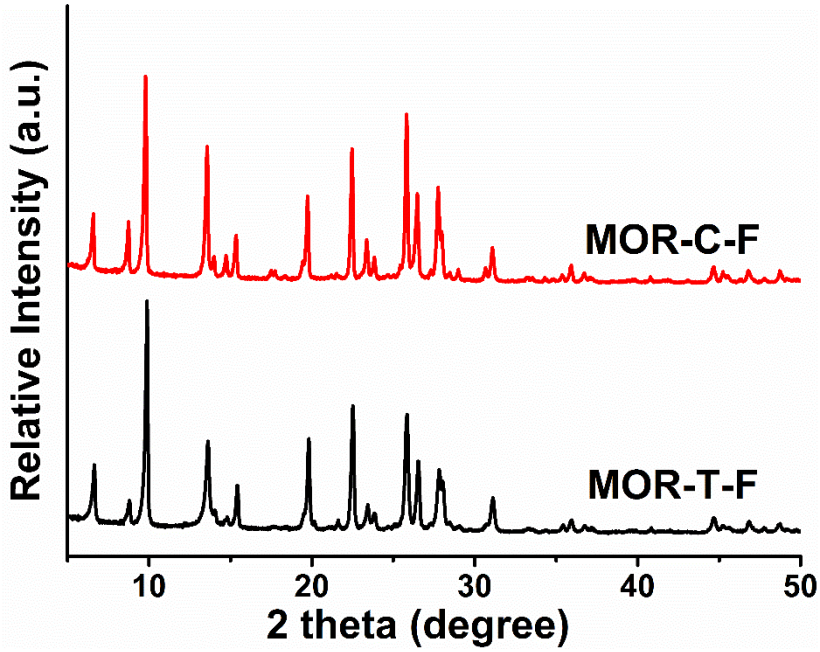

Figure S5 XRD patterns of the samples MOR-T-F and MOR-C-F prepared by chemical etching in acetone-HF acid solution.

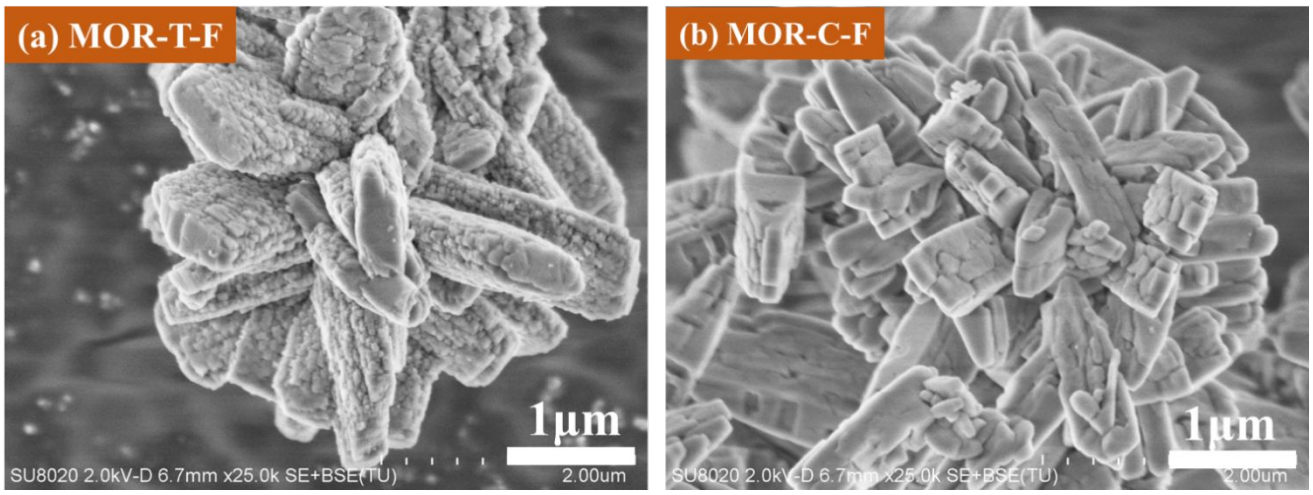

Figure S6 SEM images of the samples MOR-T-F and MOR-C-F prepared by chemical etching in acetone-HF acid solution.

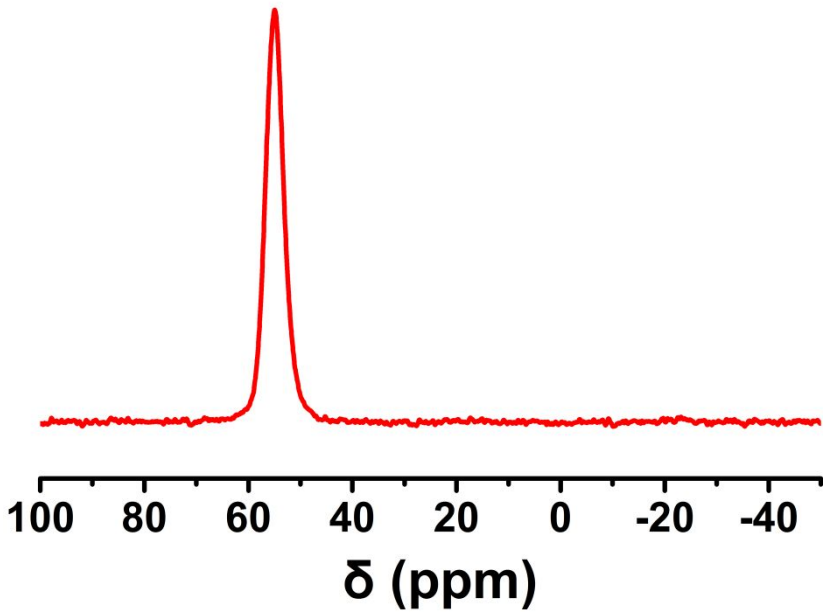

Figure S7 ^{27}Al MAS NMR spectra of the as-made sample MOR-C-F.

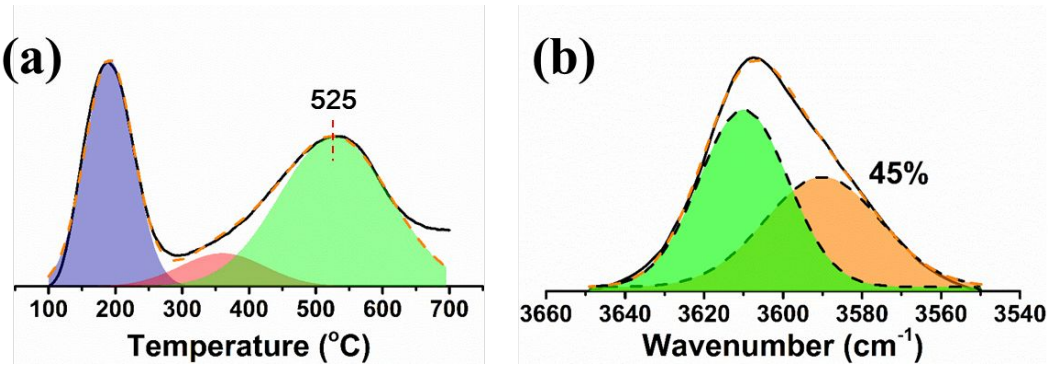

Figure S8 Acidity of the H^+-form MOR-C-F sample. (a) NH_3-TPD profile; (b) FTIR spectrum of the v(OH) region and deconvoluted bands corresponding to the acid sites in 8-MR side pockets (right) and 12-MR channels (left). The value in figure b refers to the proportion of the acid sites in 8-MR side pockets.

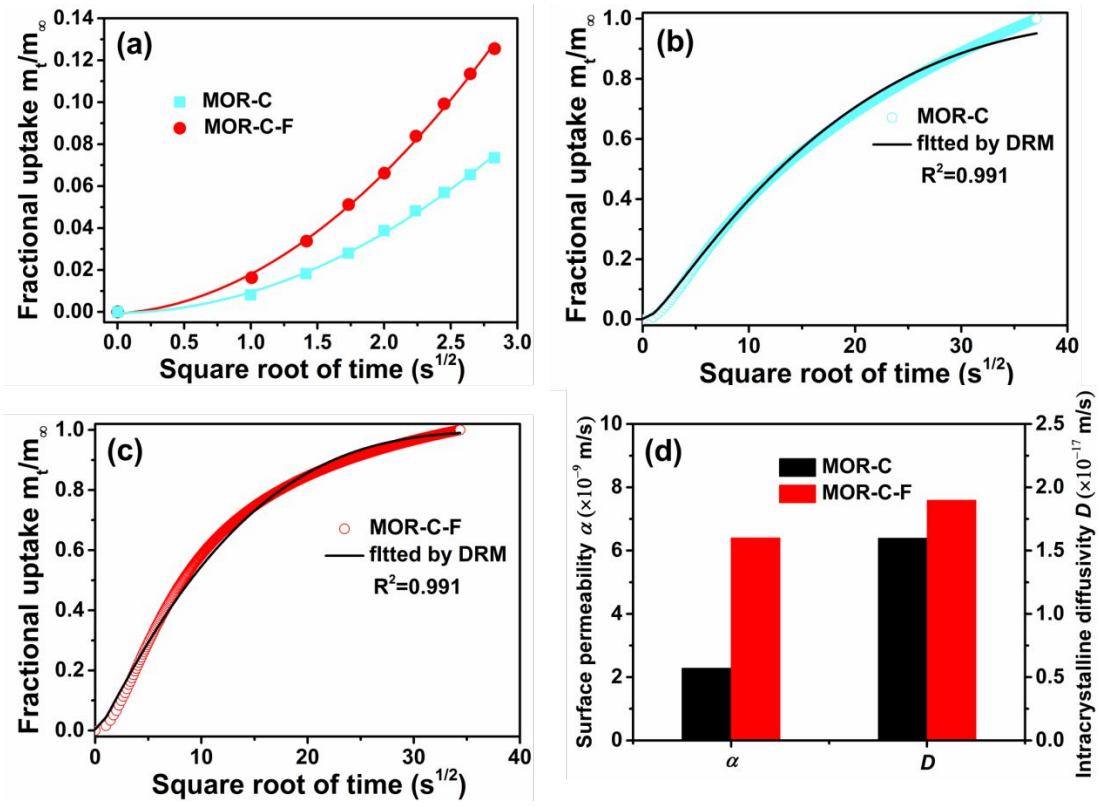

Figure S9 (a) Initial uptake rate of n-butane on H-MOR samples, at a pressure of 5 mbar, 30 °C. (b, c) IGA curves of n-butane on H-MOR samples. The scatters represent the experimental data while solid lines are fitting results by DRM. R^2 represents the correlation coefficient. (d) Surface permeability (α) and intracrystalline diffusivity (D) of n-butane derived by the uptake rates. Note that nonpolar n-butane was selected as probe molecule to reduce the interference of acid sites on diffusion.

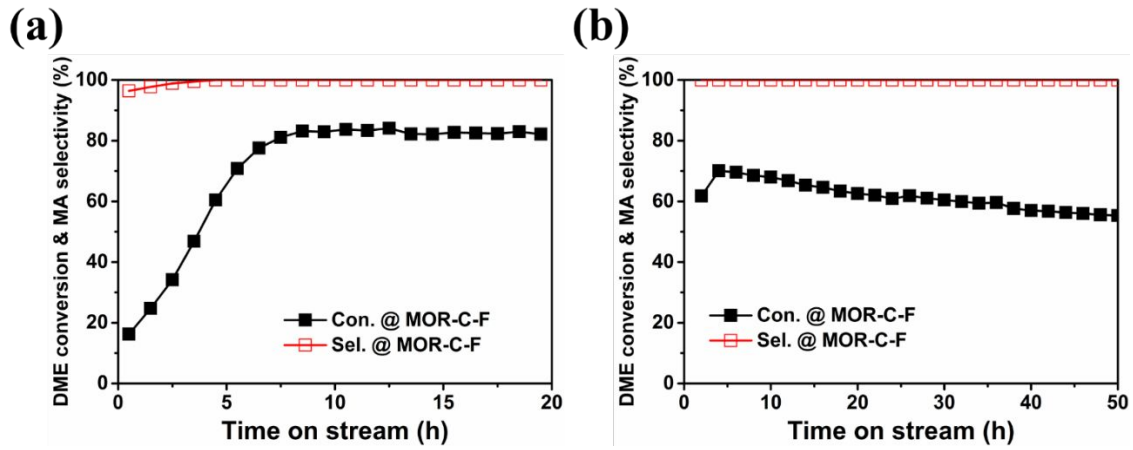

Figure S10 DME carbonylation performance over pyridine-modified H^+-form MOR-C-F catalyst. Reaction conditions: (a) 200°C, 2 MPa, DME/CO/N_2 = 5/35/60, GHSV=3600 mL/g/h. (b) 220°C, 2 MPa, DME/CO/N_2 = 5/35/60, GHSV=12000 mL/g/h.

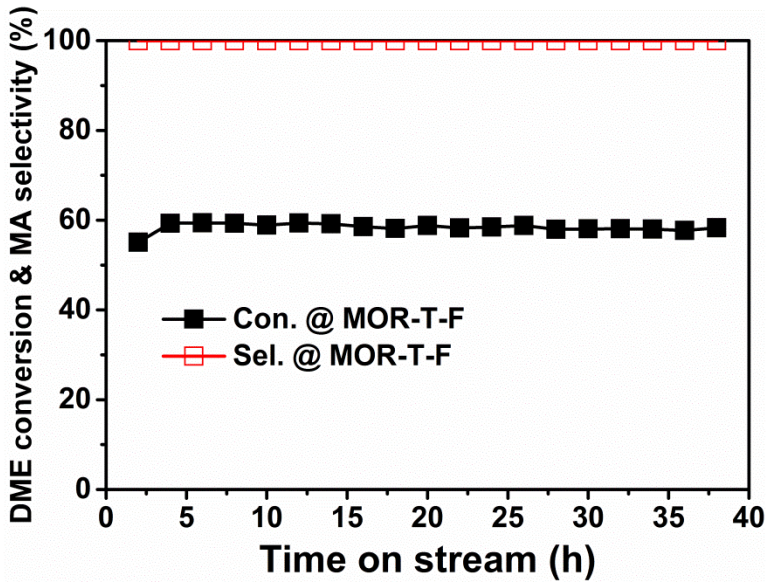

Figure S11 DME carbonylation performance over pyridine-modified H^+-form MOR-T-F catalyst. Reaction conditions: 200°C, 2 MPa, DME/CO/N_2 = 5/35/60, GHSV=3600 mL/g/h.

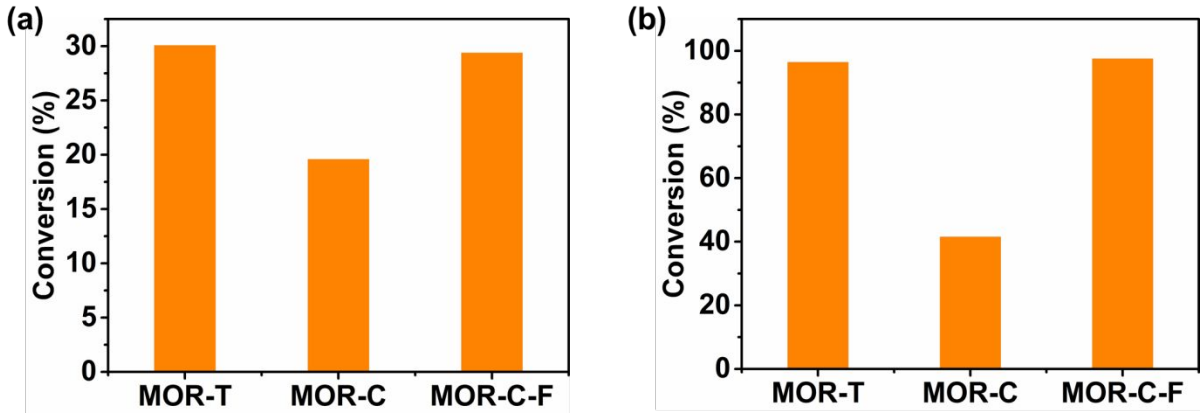

Figure S12 The catalytic cracking of hydrocarbons on MOR-T, MOR-C and MOR-C-F. (a) Isopropyl benzene (IPB) cracking versus time on stream. Reaction conditions: T = 210 °C, $WHSV_{IPB}$ = 3.4 h^{-1}, TOS = 5 min; (b) N-octane conversion. Reaction conditions: T = 500 °C, $WHSV_{n\text{-}ocane}$ = 11.6 h^{-1}, TOS = 5 min;

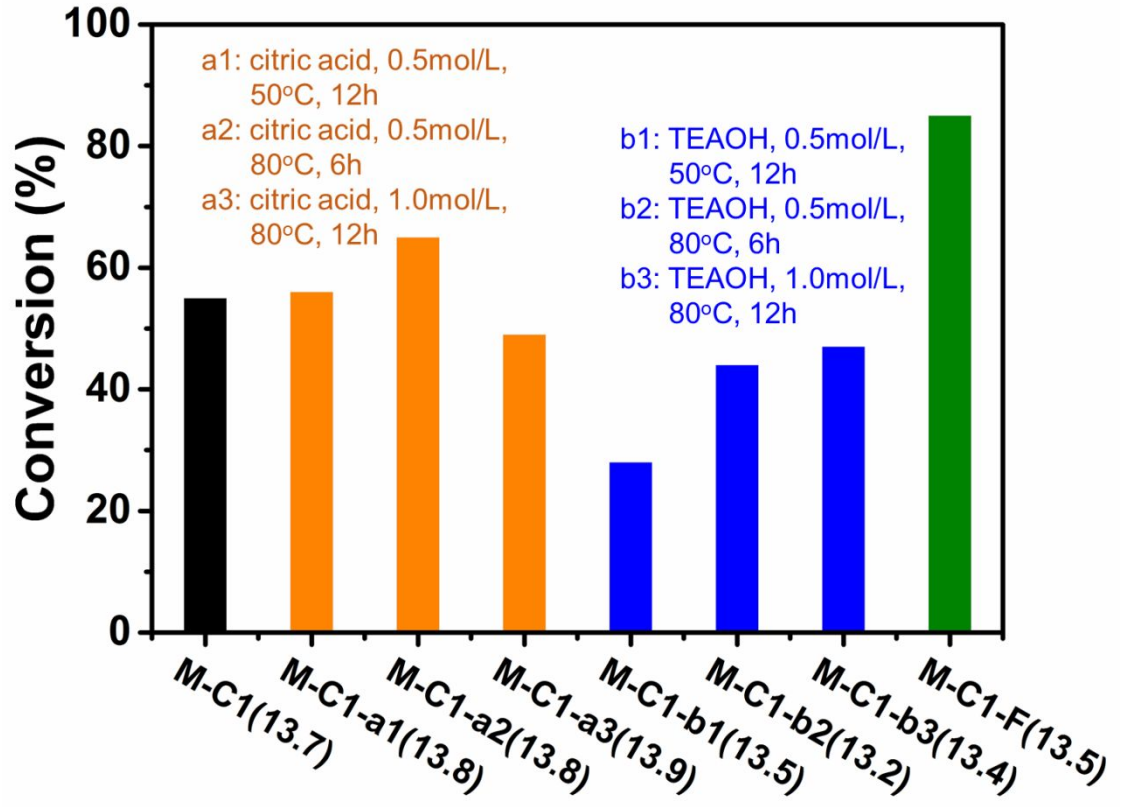

Figure S13 DME carbonylation performance over samples before and after post-synthesis treatments. MOR-C1 (sample 14 in Table S6): MOR zeolite synthesized using cyclohexylamine (CHA) as OSDA. MOR-C1-a: sample MOR-C1 after citric acid treatment; MOR-C1-b: sample MOR-C1 after TEAOH

treatment; MOR-C1-F: sample MOR-C1 after HF treatment. Reaction conditions: DME/CO/N_2=5/35/60, GHSV=3600 mL/g/h, 200 ^{o}C, 2 MPa. All the data in the figures are the conversion in the steady period.

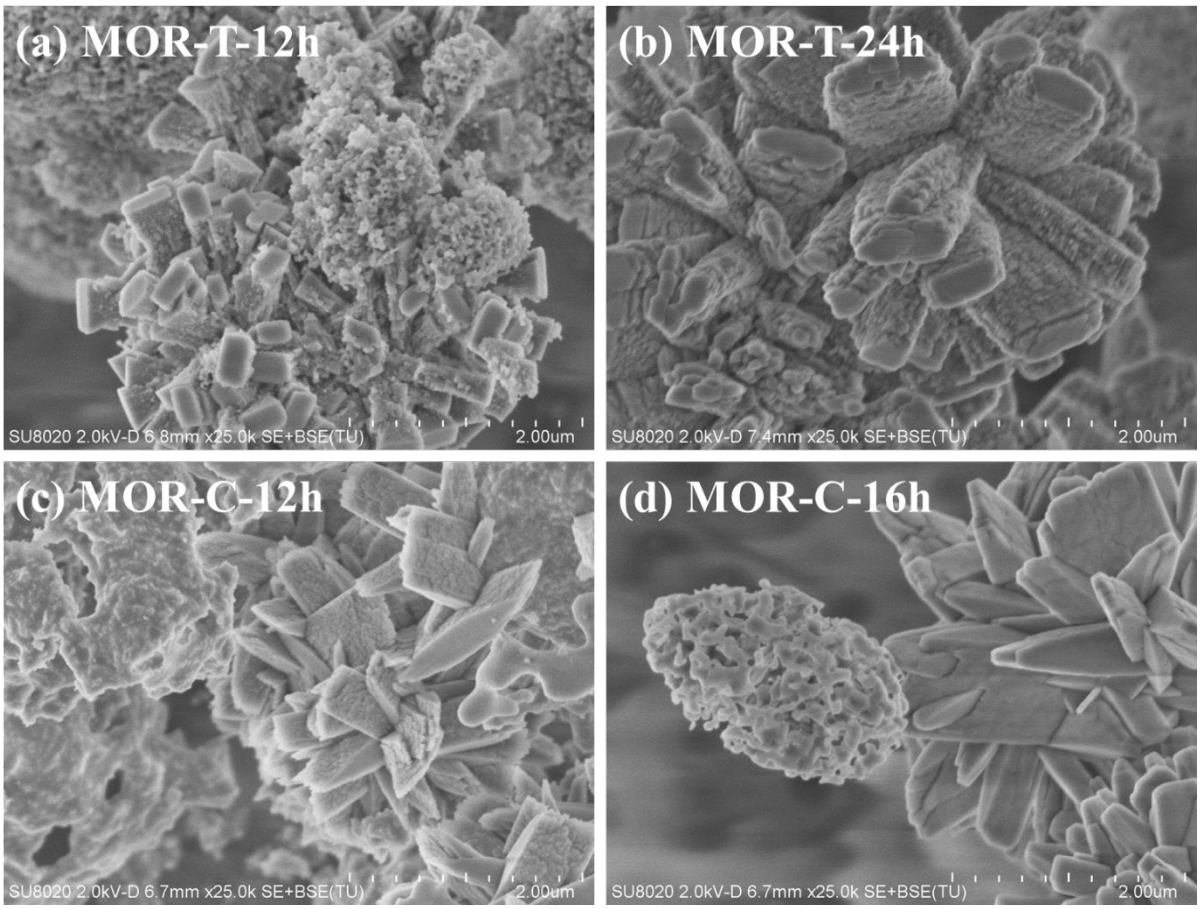

Figure S14 SEM images of the samples obtained at different crystallization times.

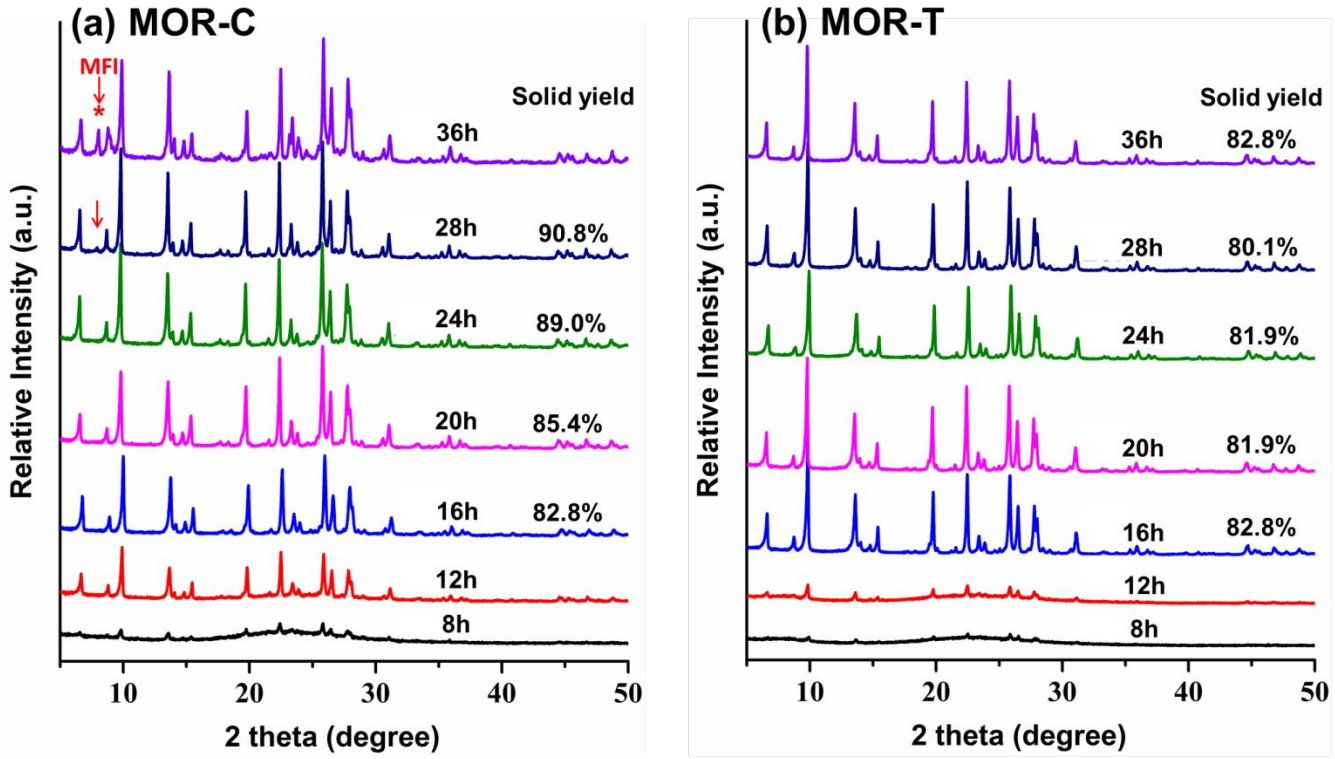

Figure S15 XRD patterns of the samples obtained at different crystallization times.

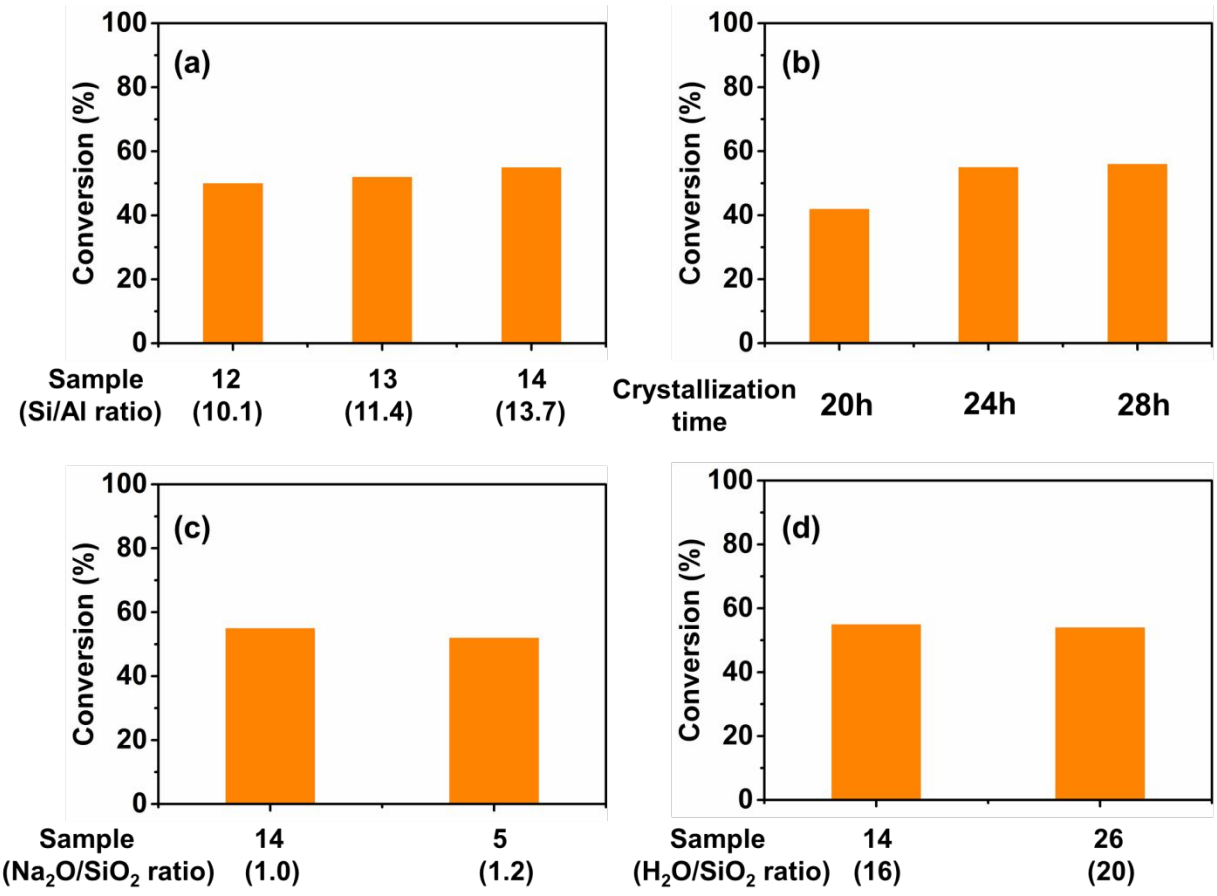

Figure S16 DME carbonylation performance over pyridine-modified H-MOR catalysts. The samples

were hydrothermally synthesized using CHA as OSDA. (a) Samples with different Si/Al ratios (the value in the bracket indicates the Si/Al ratio detected by XRF). (b) Sample 4 with different crystallization times. (c) Samples synthesized from different gel alkalinity (Na_2O/SiO_2). (d) Samples crystallized from different H_2O/SiO_2 ratios. Reaction conditions: DME/CO/N_2=5/35/60, GHSV=3600 mL/g/h, 200 ^oC, 2 MPa. All the data in the figures are the conversion in the steady period.

REFERENCES

(1) Wloch, J., Effect of surface etching of ZSM-5 zeolite crystals on the rate of n-hexane sorption. *Micropor. Mesopor. Mat.* **2003,** *62* (1-2), 81-86.

(2) Kortunov, P.; Vasenkov, S.; Chmelik, C.; Karger, J.; Ruthven, D. M.; Wloch, J., Influence of defects on the external crystal surface on molecular uptake into MFI-type zeolites. *Chem. Mater.* **2004,** *16* (18), 3552-3558.

(3) Dedecek, J.; Wichterlova, B., Co2+ ion siting in pentasil-containing zeolites. I. Co2+ ion sites and their occupation in mordenite. A Vis-NIR diffuse reflectance spectroscopy study. *J. Phys. Chem. B* **1999,** *103* (9), 1462-1476.

(4) Janda, A.; Bell, A. T., Effects of Si/Al Ratio on the Distribution of Framework Al and on the Rates of Alkane Monomolecular Cracking and Dehydrogenation in H-MFI. *J. Am. Chem. Soc.* **2013,** *135* (51), 19193-19207.

(5) Liang, T.; Chen, J.; Qin, Z.; Li, J.; Wang, P.; Wang, S.; Wang, G.; Dong, M.; Fan, W.; Wang, J., Conversion of Methanol to Olefins over H-ZSM-5 Zeolite: Reaction Pathway Is Related to the Framework Aluminum Siting. *ACS Catal.* **2016,** *6* (11), 7311-7325.

(6) Kaerger, J.; Ruthven, D. M., Diffusion in nanoporous materials: fundamental principles, insights and challenges. *New J. Chem*. **2016,** 40 (5), 4027-4048

(7) Peng, S.; Gao, M.; Li, H.; Yang, M.; Ye, M.; Liu, Z., Control of surface barriers in mass transfer to modulate methanol-to-olefins reaction over SAPO-34 zeolites. *Angew. Chem. Int. Ed.* **2020**, *59*, 21945-21948.

(8) Gao, M.; Li, H.; Yang, M.; Gao, S.; Wu, P.; Tian, P.; Xu, S.; Ye, M.; Liu, Z., Direct quantification of surface barriers for mass transfer in nanoporous crystalline materials. *Commun. Chem.* **2019,** *2*.

(9) Kim, M. Y.; Lee, K.; Choi, M., Cooperative effects of secondary mesoporosity and acid site location in Pt/SAPO-11 on n-dodecane hydroisomerization selectivity. *J. Catal.* **2014,** *319*, 232-238.

(10) Jin, D.; Ye, G.; Zheng, J.; Yang, W.; Zhu, K.; Coppens, M.-O.; Zhou, X., Hierarchical Silicoaluminophosphate Catalysts with Enhanced Hydroisomerization Selectivity by Directing the Orientated Assembly of Premanufactured Building Blocks. *ACS Catal.* **2017,** *7* (9), 5887-5902.

(11) Yue, T.; Liu, W.; Li, L.; Zhao, X.; Zhu, K.; Zhou, X.; Yang, W., Crystallization of ATO silicoaluminophosphates nanocrystalline spheroids using a phase-transfer synthetic strategy for n-heptane hydroisomerization. *J. Catal.* **2018,** *364*, 308-327.